

# Electronic Structures and Optical Properties for Nano Particles: Experimental and Theoretical Calculations

Abeer E. Aly<sup>1, 2, \*</sup>, Heba M. Fahmy<sup>3</sup>, H. H. Medina Chanduvi<sup>4</sup>, Arles V. Gil Rebaza<sup>5</sup>, B. Thapa<sup>6</sup>, A. Shankar<sup>6</sup>

<sup>1</sup>Physics Department, Higher Institute for Engineering, El Shorouk Academy, Cairo, Egypt

<sup>2</sup>Basic Science Department, Al Salam Institute for Engineering and Technology, Cairo, Egypt

<sup>3</sup>Department of Biophysics, Faculty of Science, Cairo University, Giza, Egypt

<sup>4</sup>Instituto de Fisica La Plata IFLP, CONICET La Plata, La Plata, Argentina

<sup>5</sup>Departamento de Fisica, Facultad de Ciencias Exactas, Universidad Nacional de La Plata UNLP, La Plata, Argentina

<sup>6</sup>Condensed Matter Theory Research Lab, Department of Physics, Kurseong College, Darjeeling, India

## Email address:

abeerresmat782000@yahoo.com (A. E. Aly)

\*Corresponding author

## To cite this article:

Abeer E. Aly, Heba M. Fahmy, H. H. Medina Chanduvi, Arles V. Gil Rebaza, B. Thapa, A. Shankar. Electronic Structures and Optical Properties for Nano Particles: Experimental and Theoretical Calculations. *American Journal of Nano Research and Applications*. Vol. 10, No. 1, 2022, pp. 9-13. doi: 10.11648/j.nano.20221001.12

Received: April 27, 2022; Accepted: May 12, 2022; Published: June 14, 2022

**Abstract:** The use of copper nanoparticles (Cu NPs) and copper oxide nanoparticles (Cu<sub>2</sub>O NPs) has increased dramatically both in the medical and industrial fields. In the present study, we have used various techniques like, dynamic light scattering (DLS) for particle size, zeta potential determination, X-ray diffraction (XRD), transmission electron microscope (TEM) and scanning electron microscope (SEM) for development and characterization of Cu and Cu<sub>2</sub>O NPs. We have also performed the ab-initio calculations based on the density functional theory (DFT) where the theoretical results are in well accordance with the experimental reports. The Hubbard correction is included over the generalized gradient approximation (GGA) for a better description of Cu and Cu<sub>2</sub>O NPs. The plot of densities of states (DOS) and energy band structures of Cu and Cu<sub>2</sub>O nanocrystals predicts the metallic and semiconducting nature of Cu and Cu<sub>2</sub>O, respectively. The energy bands and DOS shows strong hybridization of Cu-O and predicts the metallic nature of Cu and semiconducting nature of Cu<sub>2</sub>O. The optical absorption results show that both the Cu<sub>2</sub>O and Cu samples are absorbing strongly at the minimum energy. The band structure of Cu Nano crystals reveals a metallic nature where the valence band crosses the Fermi energy level at W point. However, an indirect energy band gap can be seen above the EF.

**Keywords:** Cu Nanoparticles, Cu<sub>2</sub>O Nanoparticles, X-ray Diffraction, Density Functional Theory

## 1. Introduction

Copper is an important trace element for energy production in biological systems. Cu nanocrystals are widely investigated for the preparation of metal oxide to study their forked properties (catalytic, sensing, electrical, and mechanical) making them suitable for various applications. They have been involved in several industrial, biological, and medical applications as they are cost effective and have simple accessibility [1]. They are also a

synthesis necessity for various enzymes, including cytochrome c oxidase, superoxide dismutase, tyrosinase, lissyl oxidase and cupro-protein [2]. Cu based compounds like copper oxide (Cu<sub>2</sub>O) NPs have been widely used in inks, lubricants, coatings, semiconductors, heat transfer fluids, antimicrobial preparations, and intrauterine contraceptive devices [3]. Ab-initio density functional theory (DFT) calculations are theoretically an appropriate tool to examine and analyze the electronic band structures and density of states of materials.

Hence, in this manuscript we present computational

analysis of Cu and Cu<sub>2</sub>O nanocrystals such as electronic structure and optical properties.

## 2. Experimental Analysis

The Cu NPs and Cu<sub>2</sub>O NPs in crystalline form were analyzed by X-ray with power of 45 KV and current of 30 mA with the scan step time of 0.5 sec at 25°C. Cu and Cu<sub>2</sub>O NPs are used in the powder form. In the process of data collections, the samples are placed on top of an aluminum slide and are widely spread to increase the exposure of X-

rays on the specified area. The Transmission electron microscopy (TEM) technique uses energetic electrons to produce crystallographic information and morphology of nanoparticles. The surface structure and chemical composition of the prepared samples are determined using Scanning electron microscopy (SEM)[4].

### *SEM and TEM of Cu NPs and Cu<sub>2</sub>O NPs*

The TEM reveals a cuboidal Cu NP shape with an average size of  $13 \pm 1$  nm, as shown in (Figure 1a). The Cu<sub>2</sub>O NPs demonstrated spherical sprinkled tiny particles with an average size of  $20 \pm 3$  nm (Figure 1b).

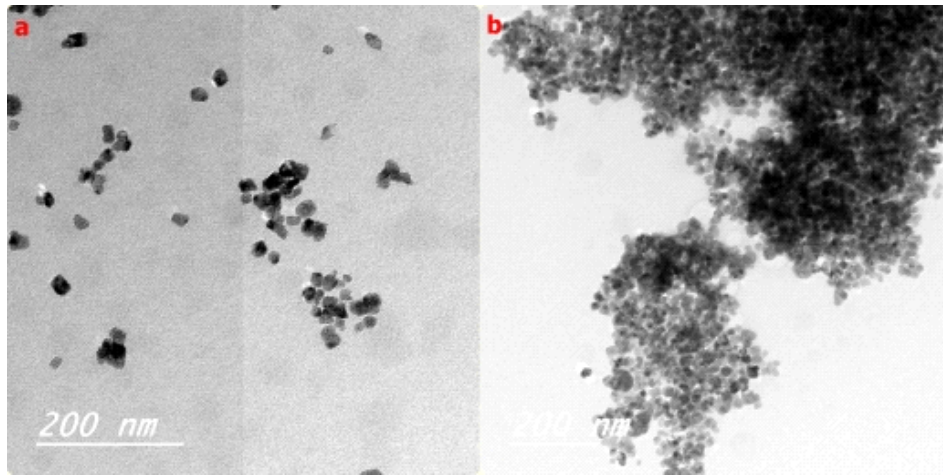


**Figure 1.** TEM micrographs of a) Cu NPs and b) Cu<sub>2</sub>O NPs.

SEM also proved that Cu NPs are cuboidal and are shown as tiny clusters (Figure 2a). The SEM image of the prepared Cu NPs is illustrated in Figure 2b, which underlines the spherical form of particle's surface.

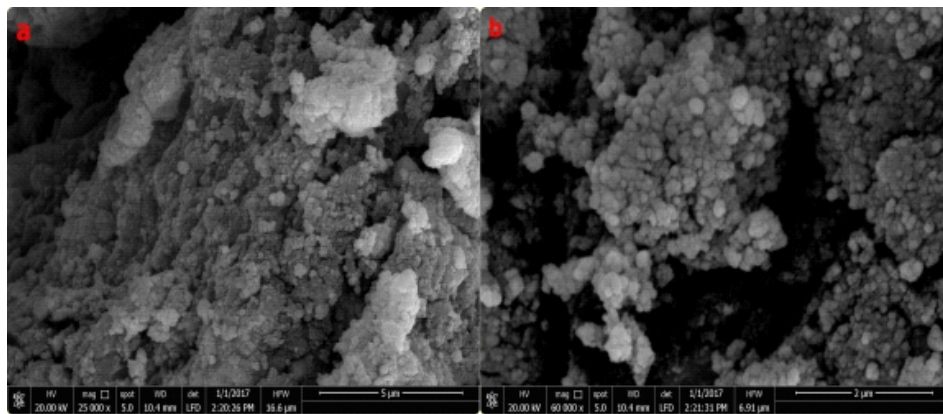


**Figure 2.** SEM micrographs of a) Cu NPs and b) Cu<sub>2</sub>O NPs.

## 3. Computational Details

Ab-initio calculation is also performed within the framework of density functional theory (DFT) [5] based on the pseudopotential and plane-wave method as implemented in the Quantum-Espresso code [6]. The projector augmented-wave (PAW) formalism is used to describe the electron-ion interactions. In contrast, the exchange-correlation terms is described using the Generalized Gradient Approximation (GGA) proposed by Perdew-Burke-Ernzerhof (PBE) [7], for

a better description of the electronic band structure of the Cu<sub>2</sub>O. GGA plus Hubbard term (U) in the self-interaction correction scheme is also applied, where the U value (U=7.0 eV) is determined using the density functional perturbed theory (DFPT). The plane-wave energy cutoff and the charge density cutoff are set to 100 Ry and 900 Ry, respectively. A 15 X 15 X 15 k-points mesh in the Monkhorst-Pack description is used to integrate the Brillouin zone (BZ), and spin polarization calculation is also considered. Optical properties are calculated using a high density of 58 X 58 X 58 k-points grid, where intra-transitions are considered [8, 9].

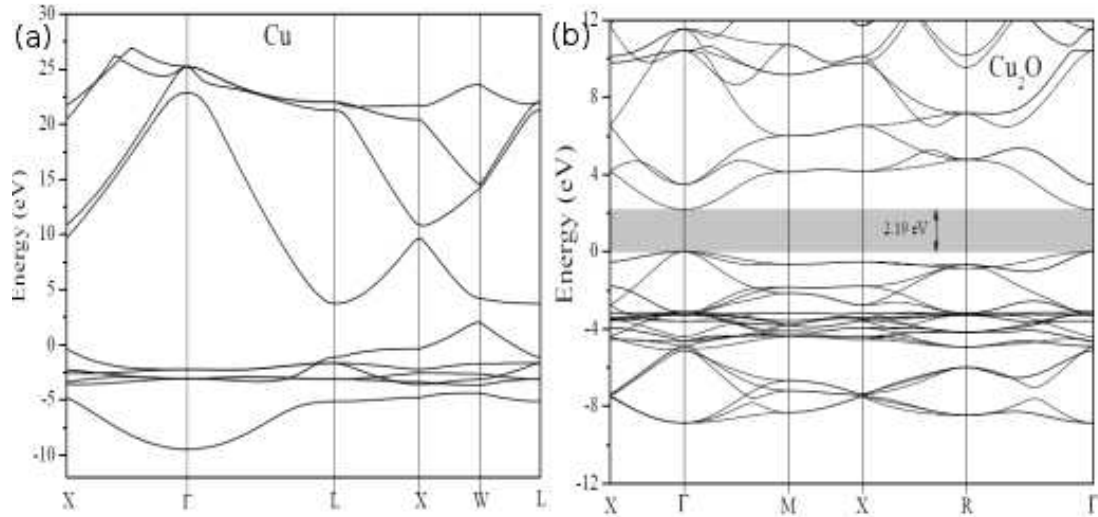


Figure 3. Energy band structure for (a) Cu and (b)  $\text{Cu}_2\text{O}$ .

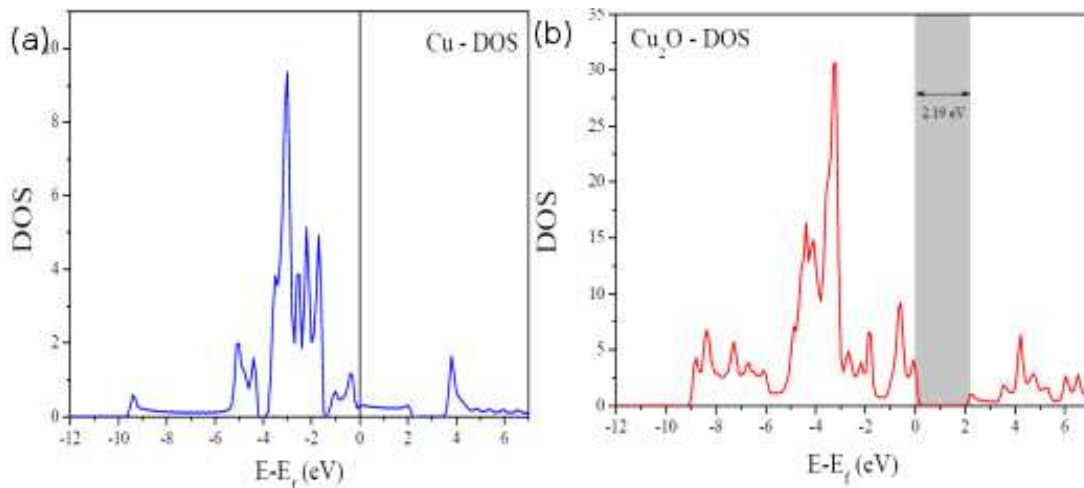


Figure 4. Total density of states (DOS) of (a) Cu and (b)  $\text{Cu}_2\text{O}$ .

### 3.1. Electronic Band Structure

In order to understand the nature of Cu and  $\text{Cu}_2\text{O}$  nanocrystals, their electronic band structure is analysed from ab initio calculations within the density functional theory, using the GGA functional. The band structure of Cu and  $\text{Cu}_2\text{O}$  nanocrystals along high symmetry directions of the Brillouin zone (BZ) are calculated and shown in Figure 3(a, b).  $\text{Cu}_2\text{O}$  is a semiconductor with a direct band gap of 2.19 eV in accordance with the experimental reports with the valence band maximum (VBM) and the conduction band minimum (CBM) lying at the  $\Gamma$  point. There exists large number of bands in the energy range of -5 eV – 0 eV indicating the hybridisation between the Cu-d and O-p states [10]. Many literature reviews reports a deviation from the experimental band gap of 2.172 eV for  $\text{Cu}_2\text{O}$  [11]. Ruiz et al. [12] obtained an  $E_g$  of 9.7 eV using a posteriori density-functional correction to the self-consistent solution to the Hartree-Fock-Roothan equation. Sieberer and collaborators [13] have reported an  $E_g$  of 0.48 eV using GGA+U, whereas

French and coworkers [14] revealed an  $E_g$  of 0.45 eV by incorporating spin-orbit coupling. However, Heinemann et al. [15] estimated an energy band gap of 2.02 eV using the hybrid functional which is in agreement with the reported value of Bruneval et al. [16]. The band structure of Cu nanocrystals reveals a metallic nature where the valence band crosses the Fermi energy level at W point. However, an indirect energy band gap can be seen above the EF.

To further elucidate the electronic band structure we have analyzed the density of states (DOS) for both Cu and  $\text{Cu}_2\text{O}$  NPs which have been displayed in Figure 4(a, b). The DOS plot of Cu revealed its metallic nature with sharp peaks arising in the energy range of -2 to -4 eV. The DOS plot of  $\text{Cu}_2\text{O}$  reflects its semiconducting nature and the Fermi energy region mostly consists of states arising from the Cu-d and O-p states [17]. At the energy range of -6 eV to -9 eV, we find states mainly composed of O-p states. Tahir et al. [18] have reported the electronic structure of bulk Cu and  $\text{Cu}_2\text{O}$  using the X ray photo electron spectroscopy method and have demonstrated a similar DOS behavior as our results for both the nanocrystals.

### 3.2. Optical Properties

To determinate optical properties, we have calculated the dielectric function  $\epsilon(\omega)$ :

$$\epsilon(\omega) = \epsilon_1(\omega) + i\epsilon_2(\omega)$$

$$\epsilon_2(\omega) = \left( \frac{\hbar e^2}{\pi m^2 \omega^2} \right) \sum_{c,v} \int d^3k \langle c_k | p^\alpha | v_k \rangle \langle v_k | p^\beta | c_k \rangle \delta(E_{c_k} - E_{v_k} - \omega)$$

The real part can be extracted from the imaginary part using the Kramers-Kronig relationship:

$$\epsilon_1(\omega) = 1 + \frac{2}{\pi} P \int_0^\infty \frac{\omega' \epsilon_2(\omega')}{(\omega')^2 - \omega^2} d\omega'$$

where P is the principal value of the integral. Knowing the real  $\Re(\epsilon)$  and complex  $\Im(\epsilon)$  part of the dielectric functional, we can determine other properties, such as refractive index, reflectivity, and optical absorption.

In Figure 5a, we show the real and complex part of the dielectric function of the Cu and Cu<sub>2</sub>O compounds. For the Cu, there are two peaks at 2.1 and 4.9 eV for the imaginary part,  $\Im(\epsilon)$ , which could be related to 3d-Cu transitions at k-points W and L, respectively. Whereas for the real part,  $\Re(\epsilon)$ , there are two peaks at 1.7 and 4.6 eV and at zero frequency limits

where  $\epsilon_1(\omega)$  and  $\epsilon_2(\omega)$  are the real and complex parts of the dielectric function, respectively. The complex part is related to the momentum matrix (p) element between occupied ( $v_k$ , valence bands) and unoccupied ( $c_k$ , conduction bands) electronic bands state  $\alpha$  and  $\beta$  with crystal momentum  $k$ ,

the value of  $\Re(\epsilon)$  is 7.5. For the case of the Cu<sub>2</sub>O, the imaginary part,  $\Im(\epsilon)$ , show two peaks at the lowest energies with respect to the Cu compound at 0.2 and 0.6 eV, related with transitions from 3d-Cu to 2p-O states, and from 4s-Cu to 2p-O states at  $\Gamma$  k-point. The real part,  $\Re(\epsilon)$ , show a negative value for a range of lowest frequencies energies, related to a metallic behavior in this frequency region. The band gap for Cu is 0 eV (metallic) and 2.1 eV for Cu<sub>2</sub>O.

In figure 5b, we show the optical absorption for the Cu and Cu<sub>2</sub>O compounds, where the optical transition for the Cu is in the visible region with a wavelength of 518 nm, corresponding to the cyan color. Whereas Cu<sub>2</sub>O is optical transitions are not located in the visible region. The optical absorption results (figure 5b) show that both the Cu<sub>2</sub>O and Cu samples are still absorbing strongly at the minimum energy shown (800 nm, or 1.55 eV).

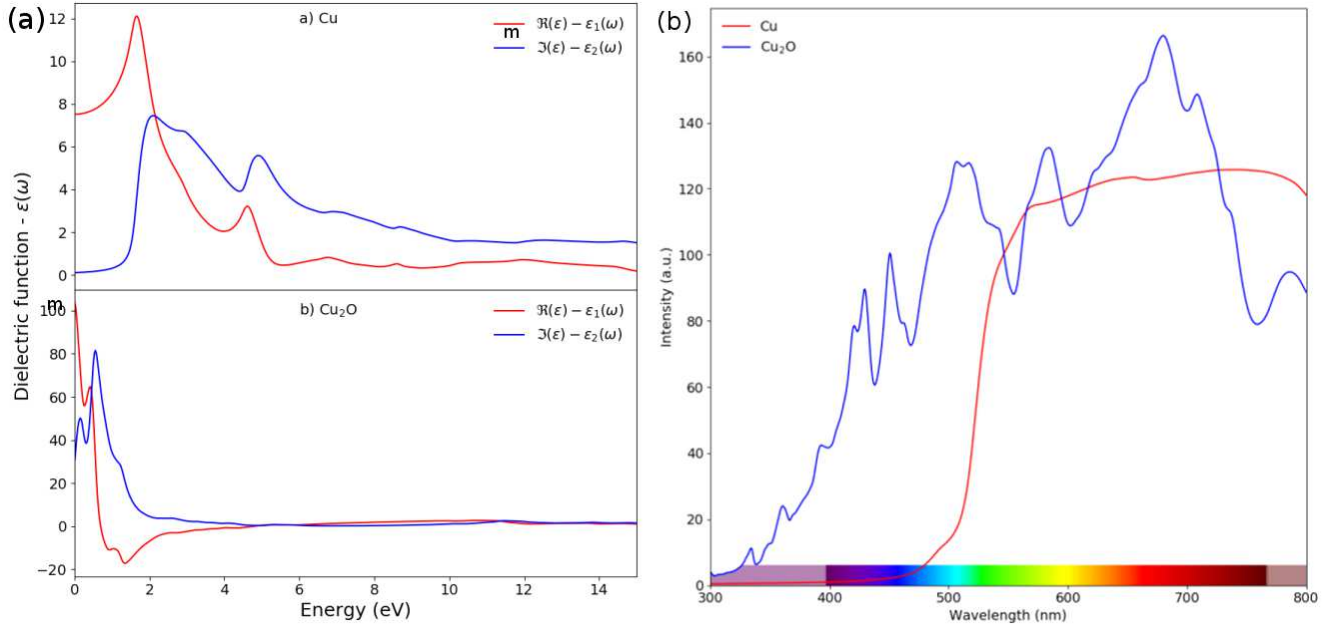


**Figure 5.** (a) Dielectric function for Cu and Cu<sub>2</sub>O compounds, (b) Optical absorption function for Cu and Cu<sub>2</sub>O compounds.

## 4. Conclusions

In this present study, Cu and Cu<sub>2</sub>O nanoparticles have been prepared, and using the first principles method, their density of states and electronic band structures have also been

investigated. The energy bands and DOS shows strong hybridization of Cu-O and predicts the metallic nature of Cu and semiconducting nature of Cu<sub>2</sub>O. The theoretically calculated  $E_g$  of 2.19 eV for the Cu<sub>2</sub>O nanocrystal is in well agreement with the experimental reports. Furthermore, the optical properties of Cu and Cu<sub>2</sub>O compounds have also been

investigated which shows an optical transitions in the visible region for Cu but reflects no optical transitions for the Cu<sub>2</sub>O compound. The optical absorption results show that both the Cu<sub>2</sub>O and Cu samples are absorbing strongly at the minimum energy.

## Author's Contributions

Heba M. Fahmy and Abeer E. Aly performed the experimental calculations, Arles V. Gil Rebaza and Dr. Abeer Esmat Aly performed the theoretical investigations, B. Thapa contributed to revise the manuscript and A. Shankar was there for evaluation of the results and is the corresponding author of the manuscript.

## No Conflict of Interest

The authors declare no conflicts of interest reported in this manuscript.

## Data Availability

The data that support the findings of this study are available from the corresponding author upon reasonable request.

## Acknowledgements

A. Shankar acknowledges the research grant from SERB, New Delhi, India (EEQ/2017/000319).

## References

- [1] Karlsson, H. L., Cronholm, P., Gustafsson, J., & Moller, L. (2008). Copper oxide nanoparticles are highly toxic: a comparison between metal oxide nanoparticles and carbon nanotubes. *Chemical research in toxicology*, 21 (9), 1726-1732.
- [2] Sternlieb, I. (1980). Copper and the liver *Gastroenterology*, 78. pp., 1615-1628.
- [3] Aruoja, V; Dubourguier, H. C; Kasemets, K. (2009). Toxicity of nanoparticles of CuO, ZnO, and TiO<sub>2</sub> to microalgae *Pseudokirchneriella subcapitata*. *SCI Total Environ*, 407, pp. 1461-1468.
- [4] Khan, M. I. Yasmeen, T., Khan, M. I., Farooq, M. and Wakeel, M., 2016. Research progress in the development of natural gas as fuel for road vehicles: A bibliographic review (1991–2016). *Renewable and Sustainable Energy Reviews*, 66, pp. 702-741.
- [5] P. Blaha, K. Schwarz, G. Madsen, D. Kvasnicka, J. Luitz, Wien2k, an Augmented Plane Wave Plus Local Orbitals Program for Calculating Crystal Properties, Technical Universität Wien, Austria, 1999.
- [6] Giannozzi, P., Baroni, S., Bonini, N., Calandra, M., Car, R., Cavazzoni, C., Ceresoli, D., Chiarotti, G. L. Cococcioni, M., Dabo, I. and Dal Corso, A., QUANTUM ESPRESSO: a modular and open-source software project for quantum simulations of materials. *Journal of physics: Condensed matter*, 21 (39), p. 395502 (2009).
- [7] J. P. Perdew, K. Burke, M. Ernzerhof, *Generalized Gradient Approximation Made Simple*, *Phys. Rev. Lett.* 77 (1996) 3865.
- [8] Evans, G. W. (1973). Copper homeostasis in the mammalian system: *Physical Rev*, 53, pp. 535-570.
- [9] X.-D. Zhou, L. R. Pederson, Q. Cai, J. Yang, B. J. Scarfino, M. Kim, W. B. Yelon, W. J. James, H. U. Anderson, C. Wang, Structural and magnetic properties of LaMn<sub>1-x</sub>Fe<sub>x</sub>O<sub>3</sub> (0.0 < x < 1.0), *J. Appl. Phys.* 99 (2006) 08M918.
- [10] Martínez-Ruiz, A., Moreno, M. G., & Takeuchi, N. (2003). First principles calculations of the electronic properties of bulk Cu<sub>2</sub>O, clean, and doped with Ag, Ni, and Zn. *Solid State Sciences*, 5 (2), 291-295.
- [11] Uihlein, C., Fröhlich, D., & Kenkies, R. (1981). Investigation of exciton fine structure in Cu<sub>2</sub>O. *Physical Review B*, 23 (6), 2731.
- [12] Ruiz, E., Alvarez, S., Alemany, P., & Evarestov, R. A. (1997). Electronic structure and properties of Cu<sub>2</sub>O. *Physical Review B*, 56 (12), 7189.
- [13] Sieberer, M., Redinger, J., & Mohn, P. (2007). Electronic and magnetic structure of cuprous oxide Cu<sub>2</sub>O doped with Mn, Fe, Co, and Ni: A density-functional theory study. *Physical Review B*, 75 (3), 035203.
- [14] French, M., Schwartz, R., Stolz, H., & Redmer, R. (2008). Electronic band structure of Cu<sub>2</sub>O by spin density functional theory. *Journal of Physics: Condensed Matter*, 21 (1), 015502.
- [15] Heinemann, M., Eifert, B., & Heiliger, C. (2013). Band structure and phase stability of the copper oxides Cu<sub>2</sub>O, CuO, and Cu<sub>4</sub>O<sub>3</sub>. *Physical Review B*, 87 (11), 115111.
- [16] Bruneval, F., Vast, N., Reining, L., Izquierdo, M., Sirotti, F., & Barrett, N. (2006). Exchange and correlation effects in electronic excitations of Cu<sub>2</sub>O. *Physical review letters*, 97 (26), 267601.
- [17] Y.-L. Lee, M. J. Gadre, Y. Shao-Horn, D. Morgan, Ab-initio GGA+U study of oxygen evolution and oxygen reduction electrocatalysis on the (001) surfaces of lanthanum transition metal perovskites LaBO<sub>3</sub> (B=Cr, Mn, Fe Co, and Ni), *PCCP* 17 (2015) 21643–21663.
- [18] Tahir, D., & Tougaard, S. (2012). Electronic and optical properties of Cu, CuO, and Cu<sub>2</sub>O studied by electron spectroscopy. *Journal of physics: Condensed matter*, 24 (17), 175002.